

Speed/Accuracy Tradeoff in Force Perception

Markus Rank and Massimiliano Di Luca
University of Birmingham

There is a well-known tradeoff between speed and accuracy in judgments made under uncertainty. Diffusion models have been proposed to capture the increase in response time for more uncertain decisions and the change in performance due to a prioritization of speed or accuracy in the responses. Experimental paradigms have been confined to the visual modality and model analysis have mostly used quantile-probability (QP) plots—response probability as a function of quantized RTs. Here, we extend diffusion modeling to haptics and test a novel type of analysis for judging model fitting. Participants classified force stimuli applied to the hand as “high” or “low.” Data in QP plots indicate that the diffusion model captures well the overall pattern of responses in conditions where either speed or accuracy has been prioritized. To further the analysis, we compute just noticeable difference (JND) values separately for responses delivered with different RTs—we define these plots as JND quantile. The pattern of results evidences that slower responses lead to better force discrimination up to a plateau that is unaffected by prioritization instructions. Instead, the diffusion model predicts two well-separated plateaus depending on the condition. We propose that analyzing the relation between JNDs and response time should be considered in the evaluation of the diffusion model beyond the haptic modality, thus including vision.

Keywords: diffusion model, force perception, haptics, JND, response time

Research on force perception dates back to Ernst Heinrich Weber (1834) and has been focused on the determination of the perceptual range and resolution of haptic perception under various experimental conditions. Force is one of the most fundamental haptic signals which is necessary for perceiving properties such as stiffness or weight. Despite its importance, experimental investigations of force sensing have focused primarily on the determination of the just noticeable difference (JND) and perceived magnitude (Jones, 1986). Few studies have however investigated the temporal aspects of haptic perception, that is, the time that is required to build up a specific percept. Exploration time, for example, has been shown to have an impact on the accuracy of shape perception (Heller, 1984; Ernst, Lange, & Newell, 2007) as longer exploration times lead to better recognition performance in a matching task. Cholewiak and Collins (2000) investigated the effects of two temporal properties, stimulus duration and stimulus onset asynchrony, on the perception of spatial direction using an array of tactile effectors attached to the body. Both temporal properties of the stimulation have an influence on the precision of the sensed direction. We are unaware of any work on the temporal characteristics of force perception.

One of the most renowned temporal characteristics of speeded perceptual judgments under uncertainty is the speed/accuracy tradeoff, the negative relation between response speed and accuracy (Luce, 1986). Such tradeoff is well studied in the visual modality, where it has been shown that the instruction about judgment speed modifies the accuracy of the responses (i.e., Swensson, 1972; Wickelgren, 1977; Ratcliff, Thapar, & McKoon, 2001; Ratcliff & Smith, 2010; P. L. Smith, Ratcliff, & Sewell, 2014; Ratcliff, 2002). Numerous studies found a speed/accuracy tradeoff in motor behavior, such as the classic Fitts's Law (Fitts, 1954) for manual pointing tasks. Several computational models from a motor control perspective have been advanced to capture this quantitative relation (for a review, see Todorov, 2004). Such a tradeoff has not yet been demonstrated for haptic judgments, and here we will do this for force perception. Different computational models have been proposed to account for the speed/accuracy tradeoff in judgment under uncertainty and most of them are based on sequential sampling of a random process (P. Smith, 2000; Ratcliff, 1978; Luce, 1986). The fundamental idea behind these models is the accumulation of noisy information over time. If the judgment is made after a long exposure to the sensory evidence, the accumulated evidence for a response is strong, allowing for a precise judgment. On the other hand, if the time for information accumulation is limited, then the intrinsic noise in the system has more influence on perception, leading to more erroneous judgments. In recent years, diffusion models have received specific attention since they can account for a large number of experimental phenomena, including visual detection and lexical discrimination (e.g., Ratcliff & Tuerlinckx, 2002; Ratcliff, 2002; Ratcliff et al., 2001; Ratcliff, Gomez, & McKoon, 2004). Current assessments for the goodness-of-fit of the diffusion model are mostly limited to quantile-probability (QP) functions, where response time quantiles are plotted over the probability of responses in a

This article was published Online First April 13, 2015.

Markus Rank and Massimiliano Di Luca, Research Centre for Computational Neuroscience and Cognitive Robotics, University of Birmingham.

We express our thanks to the anonymous reviewers and to Chris Donkin for their help on improving the manuscript's quality.

This work was supported by a fellowship within the Postdoc-Programme of the German Academic Exchange Service (DAAD) and the Royal Society research Grant RG110521.

Correspondence concerning this article should be addressed to Markus Rank, University of Birmingham, Hills Building, Edgbaston B15 2TT, United Kingdom. E-mail: markus.rank@gmail.com

specific experimental condition. While containing a huge amount of information about the participants' response characteristics, these plots are unable to capture patterns between experimental conditions such as a change in perceptual sensitivity from the instruction to focus on making a very fast or very accurate judgment.

In this article, we investigate whether the diffusion model can account for the temporal characteristics of force perception, by asking participants to make a response of whether a force applied to a gripped handle is perceived as being "high" or "low." To fit the pattern of responses with a diffusion model, we adapted the visual paradigm reported in (Ratcliff et al., 2001) to the haptic modality. In addition to assessing the goodness-of-fit with QP functions, we introduce the new notion of JND-quantile (JQ) plots, capturing perceptual sensitivity over the range of response times.

The Diffusion Model

Ratcliff's diffusion model has been shown to be able to capture the tradeoff between speed (response time) and accuracy (response correctness) of perceptual judgments in two alternative forced choice tasks in many experimental paradigms, including visual detection (Ratcliff, 2002; Ratcliff et al., 2001; Ratcliff, 1978) and recognition (Ratcliff et al., 2004). An illustration of the diffusion model is shown in Figure 1. The exposure to sensory information starts at time $t = 0$. The starting point for the information accumulation process varies at every trial and it is assumed to be equally distributed around z with a width s_z . Similarly, there is a time offset after the stimulus starts, which is uniformly distributed around T_{er} with a width s_t . The information accumulation is captured by a Wiener process $X(t)$ with drift ν and variance η^2 . The drift rate is related to the amount of information provided by the sensory stimulus over time and drives the state of the process $X(t)$ away from the initial position. There are two possible responses, R_1 and R_2 . If $X(t)$ reaches a , the "correct" answer is given (Ratcliff et al., 2001). Alternatively, response, R_2 , is initiated when $X(t) \leq 0$

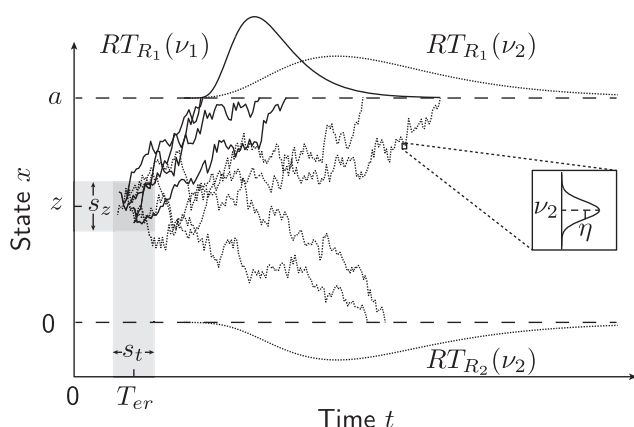


Figure 1. The diffusion model captures information accumulation in perceptual processes. Two sensory stimuli with different information content are depicted in solid and dotted lines. Sensory stimuli with more informative content ($|\nu_1| \gg 0$, solid lines) are judged faster and with a higher accuracy than ambiguous stimuli with drift rate $\nu_2 \approx 0$ (dashed lines). The distribution of response time (RT) with less informative stimuli (and with stimuli near the decision boundary) has a longer right tail.

("wrong" answer). Response time (RT) distributions are skewed and their shape depends on several factors, including the drift rate, variance, distance between the initial level and the boundary. Methods for fitting the diffusion model to experimental data are presented in (Vandekerckhove & Tuerlinckx, 2007) and implemented in the DMAT MATLAB toolbox (Vandekerckhove & Tuerlinckx, 2008).

Here we adapted the experimental task used in Ratcliff et al. (2001) to the haptic domain. In their study, participants judged whether the distance between two dots presented visually is categorized as being either "large" or "small." Two sets of instructions were given in separate blocks: Participants were either required to make a judgment as accurately as possible ("accuracy" condition) or they were given the instruction to respond as fast as they could with a time limit after which the answer was not valid any more ("speed" condition). The observed speed/accuracy tradeoff in the responses has been accounted for using a different value of a , the information needed for making a decision (see Figure 1). The distance between the two dots affected the drift rate ν such, that very large and very small distances had a large absolute drift rate that lead to a quicker decision with a higher probability of correct responses. Because our focus lies on force perception, participants in our current experiment were asked to judge whether a force applied to their hand was either "high" or "low."

Methods

Participants sat in an upright position, facing a haptic interface placed on a table. Their elbow was placed on the table surface with a 2 cm layer of cushioning material beneath. A ball-shaped endeffector of 5 cm diameter, firmly and continuously held with the right hand, conveys force stimuli toward the participant's elbow. The task was to decide whether the force is perceived as being "high" or "low." Ten force stimuli f_i^* , $i = 1 \dots 10$, evenly spaced between 2.6 N and 4.4 N were commanded to the haptic interface. The force that splits the range of forces in two equal portions is named point of objective equality (POE). Forces higher than this value are labeled as "high" forces.

In contrast to Ratcliff et al. (2001), feedback about the correct answer was given deterministically instead of probabilistic in agreement with other published works (e.g., Ratcliff & Smith, 2010). Each time the participant responded "high" to a "low" force stimulus (or vice versa) a red light-emitting diode (LED) with the label "wrong" lit up for 1 s after the response was given. For correct responses a green LED lit up instead. In addition, an orange LED lit up if the response was given after 0.7 s of stimulus presentation in "speed" trials, indicating that answers were supposed to be given faster. The next trial started 1 s after the release of the response button. Prior to experimentation, all participants were familiarized with the range of stimuli and they were instructed on how to respond to each force level.

Apparatus

The force stimuli were rendered using a force.dimension delta.3 haptic interface at a rate of 1kHz. Correct timing was ensured by using the Simulink Coder™ environment (MathWorks®) using a PC running Windows™ 7. Recorded time stamps of every simulation step guaranteed a timing accuracy of 0.001 s for the response

times. Responses were collected using the arrow keys of a customised computer keyboard where the connectors of the keys were directly wired to digital inputs of a National Instruments PCI-6229 DAQ card, controlled by the same process as the haptic rendering. Figure 2 shows a picture of the experimental setup.

Participants

Ten psychology students were recruited from the University of Birmingham and paid 15 GBP for their participation (age range = 19–27, eight female, one left-handed as assessed by a questionnaire). They all gave their written informed consent prior to participating in the study, which has been approved by the local ethics committee.

Stimuli

Force stimuli were rendered using the force profile shown in Figure 3. The force was directed toward the participant's elbow which was supported on the table to minimize movements of the arm due to the stimulus.

The onset of the force stimuli was smoothed using a third-order polynomial to overcome the inherent dynamic limitation of the haptic interface and to minimize tactile cues arising from fast-changing force stimuli. A list of 30 stimuli, consisting of three repetitions of all 10 force conditions was blocked and presented in randomized order. After every second list, participants were encouraged to take a small break; an interruption of the experimental procedure of at least 2 min was ensured after every five lists of conditions, and a break of at least 5 min after every 10 lists. Every list was repeated 25 times while participants focused on response accuracy, and 25 times while participants focused on speed; the order of lists was randomized. This led to a total of 1,500 trials which were completed in less than 2.5 h.

To verify the experimental conditions, the actual rendered force profiles were measured using an ATI Mini 145 Force/Torque sensor connected to the DAQ card. Force profiles for all experimental conditions were recorded with five repetitions at three different locations within the workspace of the haptic device. A constant, rigid contact between the handle and a wall ensured the elimination of any relative movement between device and the sensor. Although the measured force profile did not show appreciable differences with the instructed profile in terms of the force rise time, differences in the force plateau could be distinguished

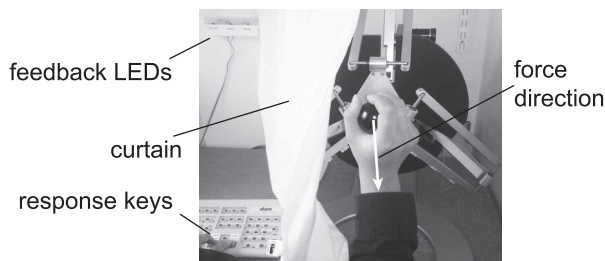


Figure 2. Force stimuli were rendered using a 3 *df* haptic interface. Forces were aligned with the participant's forearm and directed toward the elbow to prevent any movement that could affect the discrimination of force magnitude.

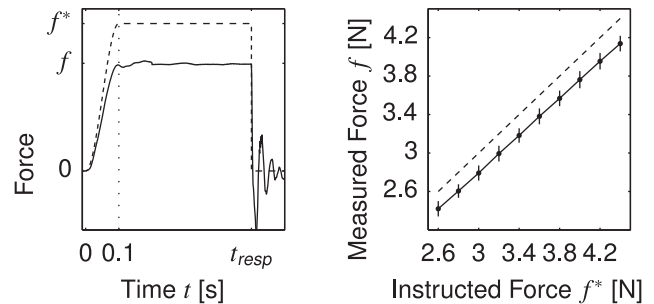


Figure 3. Left panel: Force stimuli were step-like functions whose onset was smoothed by a third-order polynomial. The force actually produced by the haptic device deviates from the commanded force as indicated by the discrepancy between the measured force (solid line) and the commanded force (dotted line). Right panel: Force measured 0.3 s after onset is on average lower than the commanded value for each of the force stimuli employed in the experiment. The values identified by a regression line are used in the paper. Error bars indicate the standard error of the mean of 15 sample measures.

clearly. The differences between the instructed forces and the measured ones is summarized in Figure 3. The measured (stationary) force f for each of the instructed forces f^* has been approximated by the regression function

$$f_{mea} = 0.96 f^* - 0.08 \text{ N}$$

obtaining a correlation coefficient of $R^2 = 0.98$. In the following sections, all analyses are based on the measured force levels, being 2.4 N, 2.6 N, 2.8 N, 3.0 N, 3.2 N, 3.4 N, 3.6 N, 3.8 N, 4.0 N, and 4.1 N. Consequently the POE splitting the range in two is 3.3 N.

Results

Response times are normalized by performing a logarithmic transformation (Ratcliff, 1993) and trials that deviate more than 3 *SDs* from the mean (separately for “speed” and “accuracy” condition for each participant) are identified as outliers (0.9% of all responses). Responses are faster in the “speed” condition than in the “accuracy” condition (paired sample *t* test on the transformed RT values $t(9) = 3.74, p < .01$).

Responses given very fast are sometimes not based on sensory evidence but are only guesses or a “startle” process. In previous research, these responses have been accounted for by introducing a lower threshold on response times before modeling with a diffusion process (Ratcliff & Tuerlinckx, 2002; Vandekerckhove & Tuerlinckx, 2007; Ratcliff, 1993; Vandekerckhove & Tuerlinckx, 2008; Ratcliff & Smith, 2010). To identify these fast guesses, we consider the easiest force condition and analyze the probability of correct responses within time windows of 0.05 s length as depicted in Figure 6 (right). For each individual participant, the threshold response time leading to more than 80% of correct responses is identified as a lower bound and responses earlier than this are excluded from the diffusion modeling.

A joint visualization of RT as a function of the probability of responses is the so-called QP plot (Ratcliff, 2002; Ratcliff et al., 2001, 2004; Ratcliff & McKoon, 2008; Ratcliff & Smith, 2010) where we will use a form of visualization plotting the probability to respond “high” and the probability to respond “low” separately

(as in Ratcliff & McKoon, 2008). We will discuss the general components of the representation and refer to Ratcliff and Smith (2010) for a comprehensive discussion. Response times are separated into “high” and “low” responses, sorted and binned in the fastest 10%, 30%, 50%, 70%, and 90% response time quantiles as illustrated in Figure 4. RT quantiles are then plotted for every force magnitude as a function of probabilities p_{high} to respond “high” and p_{low} to respond “low.” QP functions are shown in Figure 5 separately for the “speed” and “accuracy” conditions. It can be seen that the 10% quantile is approximately constant, regardless of the probability of “high” and “low” responses. This means, that the fastest answers are given at a minimum time which is unaffected by the stimulus condition. Differences between experimental conditions are evident in the 70% and 90% RT quantiles: Conditions with a response probability near 0.5 (that means, where participants guessed whether a high or low force was presented) tend to be slower in these percentiles. Response time distributions for force levels near the PSE thus have the same onset as the ones on the extreme ends of the tested range, but longer tails.

The probability of “high” responses over the stimulus force level is depicted in Figure 6 (left). Cumulative Gaussian distributions are fitted to the experimental data separately for each participant using the Bayesian inference method (Wichmann & Hill, 2001). The point of subjective equality (PSE) corresponds to the force level resulting in a 0.5 probability of “high” responses. The JND is defined as the force difference between the force corresponding to the 0.75 probability and the PSE. PSE values for the

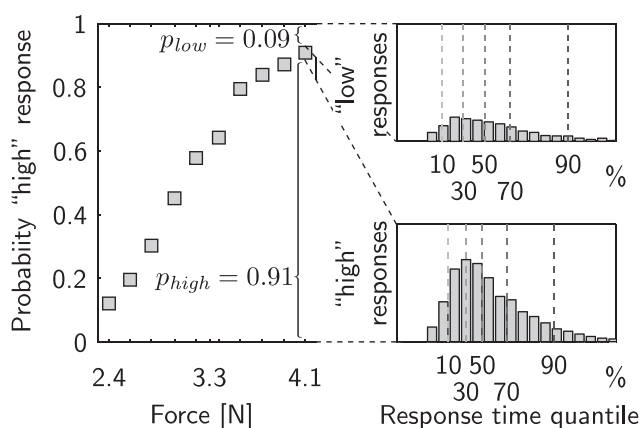


Figure 4. Every force stimulus has two possible responses (“high” and “low”) that when averaged across trials lead to the probabilities p_{high} and p_{low} , respectively (left). For one participant, the probability of responding “high” as a function of force increases from low to high force stimuli, with a slope that represents the sensitivity (see Figure 6). (right) The two inserts show response time distributions for one force stimulus (4.1 N) separated for the two types of responses. The dotted lines represent 5 quantiles (10%, 30%, 50%, 70%, 90%), which are calculated separately for each type of response and stimulus. Reaction times are higher (i.e., longer right tail) for the less-frequent (and wrong) “low” responses. From this data, two types of representations can be obtained. Quantile-probability plots (see Figure 5) are obtained by plotting the five response time quantiles as a function of the two probabilities of response for each stimulus level. To calculate just noticeable difference-quantile plots (see Figure 7), instead, the 5 quantiles are used to separate the data and then fit a psychometric function for each quantile (as shown on the left side of Figure 6).

“accuracy” and “speed” conditions are 3.16 ± 0.04 N (mean \pm SEM) and 3.17 ± 0.05 N. These values are significantly lower than the 3.3 N POE (one sample test $t(9) = -3.82$, $p < .01$; $t(9) = -2.86$, $p < .05$) and they do not differ according to the condition (paired sample t test, $t(9) = 0.16$, $p = .88$). However, the PSE values are almost coincident with the stimulus nearest to the POE (3.18 N).

JND values indicate a higher sensitivity to force in the “accuracy” condition, 0.36 ± 0.05 N than in the “speed” Condition 0.57 ± 0.1 N (one-tailed t test $t(9) = -2.14$, $p < .05$). To be able to capture the temporal properties of such sensitivity values analogously to the QP function, here we perform a new type of analysis that we define as JQ plot. Participants’ responses are split according to the RT quantile and a psychometric function is fitted to the data from each subdivision. JNDs are estimated separately from data between the 0% and 10% quantile of the RT distribution as well as from data between the 10% and 30%, 30% and 50%, 50% and 70%, and the 70% and 90% quantile. The values obtained in the “speed” and “accuracy” conditions are depicted as a function of the RT for that quantile in Figure 7. We discuss JQ functions with and without the identified fast guess responses as discussed above. A two-way repeated-measure analysis of variable on JQ data including fast guesses with factors quantile and condition reveals a significant change in JND as a function of time, but not instruction ($F(4, 36) = 3.68$, $p < .05$; $F(1, 9) = 4.81$, $p = .055$). The interaction between the two factors is not significant, $F(4, 36) = 1.1$, $p = .38$. A linear regression analysis on the JND over RT quantile reveals a slope which is significantly different from 0 in the “speed” condition, $t(9) = -2.8$, $p < .05$ but no significant trend in the “accuracy” condition, $t(9) = -0.85$, $p = .42$.

Parameters for the diffusion model (Ratcliff, 1978; Ratcliff & Tuerlinckx, 2002; Ratcliff, 2002; Ratcliff et al., 2001) are identified using the DMAT Toolbox for MATLAB (Vandekerckhove & Tuerlinckx, 2007, 2008) for every individual participant (see the Appendix). The model parameters (see Figure 1) are constrained to be identical across the various experimental conditions except for:

1. the boundary separation a that varies between the speed and accuracy instructions,
2. the initial state of the diffusion model z , and
3. the drift rate’s mean ν being proportional to the force level.

The predictions of a numerical approximation of the diffusion model (Ratcliff & Tuerlinckx, 2002) with the identified parameters is shown in the QP plot of Figure 5. The values in the JQ plot in Figure 7 are instead obtained by fitting a psychometric function to 1,000 simulated trials from the diffusion model with the identified parameters.

Discussion

Results indicate a consistent difference between the PSE and the POE across participants. This difference could be explained by appealing to the nonlinear perception of force magnitude, such as the commonly reported power function (Jones, 1986). It is expected that participants infer the force level separating “high” and

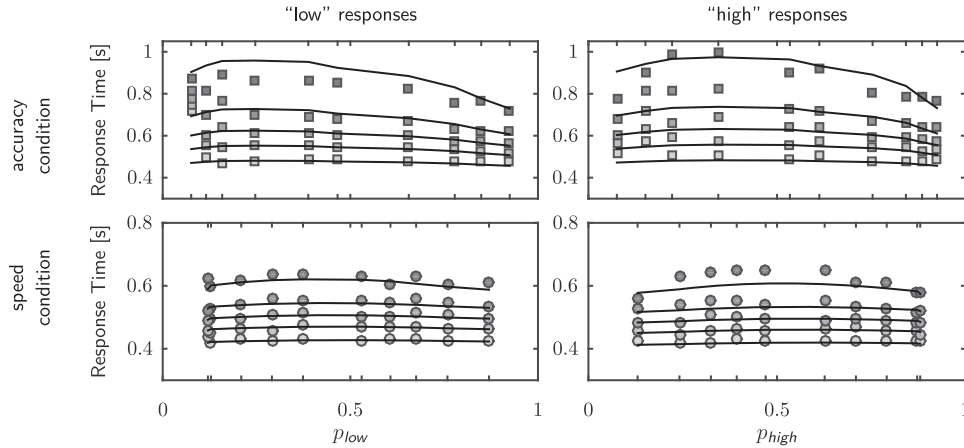


Figure 5. Quantile-probability (QP) plots averaged across participants (shaded symbols) and predictions of the diffusion model after parameter identification (lines). “Accuracy” and “speed” prioritization conditions are displayed separately in two rows. The data is also separated in two columns depending on the response (“low” and “high”). The five response time (RT) quantiles (as shown in Figure 4 for one participant) are depicted from light to dark gray as a function of average probability of response (p_{high} and p_{low} , respectively). The QP plot highlights how response time increases for force level stimuli that lead to an equal number of “high” and “low” responses (data is situated in the middle of the horizontal axis). The pattern is however asymmetrical with slower RTs for responses that are less numerous for a given condition (situated in the left portion of the horizontal axis). The diffusion model captures these two features well as evidenced by the similar pattern of lines and symbols. QP plots allow to see that the “accuracy” and “speed” conditions lead to different pattern of responses, with slower responses on the top row, but probability values that are more spread along the horizontal axis suggesting better discrimination of force level. However, QP plots do not allow quantitative comparisons of performance (as possible with just noticeable differences shown in Figure 6) nor allow the analysis of sensitivity as a function of RT.

“low” forces in two equal intervals by estimating the middle point of the perceived force range, rather than the physical force range. Because PSEs are smaller than the POE, this means that participants overestimated smaller forces and underestimated large ones. This is consistent with a power function with an exponent between 0 and 1, which is in the range of exponents reported for haptic tasks (Jones, 1986).

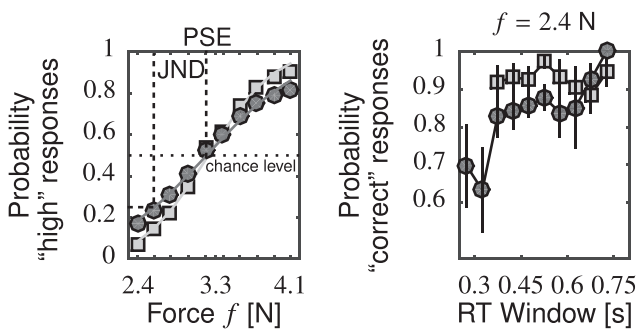


Figure 6. Left panel: Psychometric functions for “accuracy” (light gray, square) and “speed” (dark gray, round) conditions for data pooled across the 10 participants (right panel). Conditional accuracy graph for the lowest force stimulus $f = 2.4$ N in the two conditions. The graph is obtained by plotting the probability of correct responses as a function of response time (RT) binned in 0.1s windows. Responses given with a response time less than 0.4 s do not significantly deviate from chance level. PSE = point of subjective equality.

QP Plots

The QP plots in Figure 5 exhibit typical features of a speed/accuracy tradeoff which is also found in similar studies on visual perception (Ratcliff et al., 2004; Ratcliff & Smith, 2010; Ratcliff et al., 2001; Ratcliff, 2002). Responses are faster in the “speed” condition, but discrimination is better in the “accuracy” condition. All QP plots show an inverse U-shape where the curvature of the shape gets more pronounced with higher quantiles, the U-shape is generally more noticeable in the “accuracy” condition. This seems to indicate that participants tend to take more time when the judgment is difficult as the probability to respond “high” or “low” is near the chance level, in line with what has been found in the visual modality. The difference between the two experimental instructions is evident from the time values of the 90% quantile—while almost all responses were given within 0.7 s after the stimulus onset in the “speed” condition, participants took longer in the “accuracy” condition. This is irrespective of the 10% quantile being similar for both experimental manipulations. We may partially associate the latter result to the censoring procedure applied to eliminate fast guesses, since this affects predominantly the responses in the “speed” instruction (Figure 6, right panel).

JQ Plot

QP plots contain detailed information about the response time distributions for correct and erroneous responses. The distributions are plotted as a function of the averaged probability of responses across the whole condition. In doing so, there is the assumption

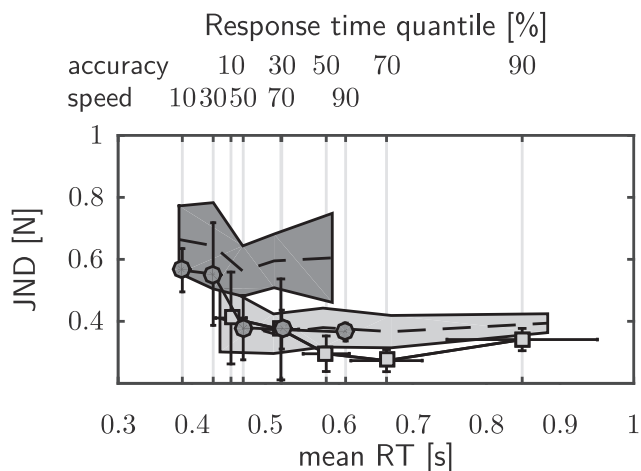


Figure 7. Just noticeable difference (JND)-quantile (JQ) plots are obtained by plotting JNDs (see Figure 6) obtained with data separated in response time (RT) quantiles (see inserts of Figure 4) over the respective quantile's mean RT. The “speed” condition is marked by dark circles, the “accuracy” condition by light squares. The data of the two conditions evidence a decrease in JND with slower responses until values reach a plateau (performance ceiling). The pattern of the two prioritization conditions are largely overlapping, suggesting similar discrimination performance when RT is considered. This empirical data is compared to JND values obtained from the data of the diffusion model shown in Figure 5 which is marked with dashed lines inside the shaded areas (dark for the “speed” condition and light for the “accuracy” one). The two areas are largely separated, suggesting that the diffusion model predicts different task sensitivity depending on prioritization instruction. Error bars and shaded areas represent *SEM* across participants.

that responses and thus their precision are independent from their response time (quantiles are plotted vertically aligned). In the JQ plot, on the other hand, force level conditions are combined to capture performance separately for responses given with different delays. In other words, the JQ plot can evidence the pattern of speed/accuracy tradeoff rather highlighting the difference in response time for each force stimulus condition as in the QP plot. In a similar way, the conditional accuracy function (as discussed, e.g., in Luce, 1986, p. 236) as an empirical representation of the speed/accuracy tradeoff could theoretically capture related patterns. However, to represent our current data, we would have to plot one conditional accuracy function for every force level and for every instruction (“speed”/“accuracy”), leading to a total of 20 individual functions, making an intuitive interpretation rather difficult. Moreover, to obtain a compact representation of the speed/accuracy tradeoff using conditional accuracy functions requires the control of the number of errors the participant makes, otherwise this could lead to problems in visualization (Bonnet & Dresch, 1993). An example of such problems is the ceiling effect as visible in the “accuracy” condition in Figure 6 (left) where responses are always correct independently of the time taken to respond. The JQ plot does not have this limitation as it can capture patterns in the data with several levels of the independent variable, for example, the seamless transition between fast and accurate responses that would be harder to see in RT distributions for correct and error responses or individual conditional accuracy functions.

In Figure 7 we show JND over response time quantile for “speed” and “accuracy” conditions discarding the fast guess responses to make a fair comparison between model predictions and experimental data. The results from the regression analysis indicate that judgment accuracy depends on the response delay (especially in the “speed” condition): The later the response is given, the more accurate is the judgment. The decrease in performance at low RTs is due to the presence of fast but random responses, as shown in Figure 6 (right). Another possible explanation for this pattern is that the stimulus intensity is the dimension to be judged, whereas this seldom happens in visual experiments (visual intensity is often orthogonal to the property under scrutiny). Force stimuli are also inherently time-varying (they always rise from 0 N to the respective force stimulus level in 0.1 s). But as participants anticipate the stimuli's onset time, the stimulus rise-time could lead them to respond “low” shortly after the expected force onset, irrespectively of the actual stimulus presented. The data pattern suggests that such type of answer happens only for very fast responses. Instead, after 0.6 s the judgment accuracy does not improve further by accumulating additional information.

A second difference between JQ and QP plots is the ability to jointly visualize “speed” and “accuracy” conditions. In this way, it is possible to detect that the JND values for the “speed” and “accuracy” condition overlap substantially so that the “accuracy” curve seems to extend the “speed” curve toward longer RTs. Irrespective of the experimental instructions, additional time to responds improves the quality of responses until RTs reach 0.6 s. This suggests that the perceptual sensitivity reaches a maximum performance and additional decision time does not help. Interestingly, we observed such a phenomenon also in a similar study, where participants move their hand instead of keeping it static (Rank & Di Luca, 2014). Although we did not include a “speed” condition in Rank and Di Luca, 2014), the different movements caused the JND to differ only at fast response times, but the values were not influenced by the experimental manipulation for responses given after ~650 ms.

These results suggest a robust relation between sensitivity and RT in force magnitude perception which is independent of prioritization instructions. Somewhat opposite to the idea of the diffusion model where reaching a decision boundary determines the RT, here it seems that the prioritization of a fast response requires participants to give a response using the information acquired, thus limiting the response quality. We speculate that in the data analyzed there are two mechanisms involved: one limiting perceptual sensitivity in fast responses and another in slow responses. It is still to be determined whether this phenomenon is unique to the stimuli used and to the haptic modality or it is ubiquitous across sensory systems. In haptics, such duality in temporal sensitivity might be connected to the presence of mechanoreceptors with different in temporal characteristics. Whereas Meissner corpuscles fire for fast-changing forces, Merkel disks react slowly to force stimuli (Lederman & Klatzky, 2009). In vision there is a similar dualism as two separate processing streams exist—the parvocellular (P-) and magnocellular (M-) visual pathways (Livingstone & Hubel, 1987)—and this can lead to marked differences in tasks involving spatial and temporal properties.

Diffusion Model Fit

Predictions of the parameterized diffusion model are depicted in Figures 5 and 7. Parameter values for the diffusion model are summarized in the Appendix (see Table A1). Compared to the visual experiment that motivated our study, we had to include a nonzero value for the variability in the nondecision time s_i to achieve a good fit. With $s_i = 0$, the fit obtained had goodness-of-fit values of $\chi^2 \geq 500$ for all participants. A possible reason why a parameter $s_i \neq 0$ was needed could be found in the smooth onset of our force stimulus. It has been shown (Ratcliff, 2002) that all parameters of a modified diffusion process with time-variant drift rate rising from 0 to a constant level can be successfully recovered except for an increase in s_z , T_{er} , and s_r . The shape of the predicted and experimental QP plot data in Figure 5 is similar. The χ^2 measure of fit has a critical value of 231.8 to indicate a significant difference between model and data with $p = .05$, given our fitting method with 198 degrees of freedom. In our case, eight out of ten participants stay below this critical value, indicating a reasonable good fit which is comparable to the one found in (Ratcliff et al., 2001). The model parameters fitting our haptic data differ in some ways from those found in Ratcliff et al. (2001): First, the nondecision time T_{er} seems remarkably large with 0.44 s, whereas the 0.1 RT quantile in the “speed” condition is only slightly higher than in the reported visual study. We could associate this large value with a potential time-varying drift rate at the force onset, as discussed above. However, $T_{er} - 0.5 s_i$ is smaller than the 10% quantile which indicates a reasonable match between model and data. The range of drift rates between -0.36 and 0.42 is in the range of values reported in other studies as well. The mean drift rate at the POE is 0.028 , thus slightly larger than 0, leading to a tendency to respond (“high”) in this (virtual) condition. This coincides with our finding from the psychometric function, suggesting that forces are generally overestimated in the task described here, leading to a PSE which is smaller than the POE.

We attempted to further increase the goodness of fit with several model variations.

- Force magnitude perception has been reported to follow a power function (Jones, 1986). We identified the exponent of a power function for each individual participant from freely identified drift rates and used it to fit the model.
- Haptic perception is known to follow Weber’s Law (Weber, 1834); the accuracy of a force perception judgment depends on the magnitude of force applied. A linear increase in the standard deviation of the Wiener process η could account for such behavior.
- The polynomial smoothing of the force onset could affect the start of the information accumulation T_{er} . Assuming the force exceeding a (constant) absolute detection threshold triggers the information accumulation process, T_{er} would evolve approximately reciprocal with the magnitude of the target force f .

None of the modifications improved the fit above significance in a likelihood ratio test for more than two participants.

Instead, the pattern of results has a notable deviation from the predicted evolution of the JQ plot. While the experimental data evidences a steep decrease in JND for small RT in the “speed” condition, the curves obtained from the diffusion model simulation

are much flatter. This could be due to the absence of that fast error responses in the model fitting.

There is a second, more critical aspect of the model which becomes evident when inspecting the JQ plot. The data obtained from the fitted diffusion model does not capture the fact that JND curves of the “speed” and the “accuracy” conditions overlap when RTs are in a similar range and both curves appear to converge to a lower bound. The diffusion model postulates a specific threshold a for the information accumulation process to terminate causing nonoverlapping data in the JQ plot for the two conditions. In the reported studies, a could be influenced by the instruction given to focus either on the time or the accuracy of the judgment. Finding overlapping patterns of data in the JQ plot over different instructions suggests a common perceptual mechanism for the decision making process instead of a discrete threshold value for each condition.

Alternative Models

Accounting for the observed pattern of data in the JQ plot must capture the smooth transition between “speed” and “accuracy” condition. One possibility is a decision criterion $a(t)$ changing its value over time. When decisions are made early, less information is to be accumulated, later more information is taken into consideration to make a (precise) judgment. The drawback of this modification is that response times are likely no longer inherently predicted by the model, but a preference whether to respond early or late must be assumed a priori to parameterize $a(t)$. Our previous assumption of different values for a is in line with previous findings (Ratcliff et al., 2001; Vandekerckhove & Tuerlinckx, 2007; Ratcliff, 2002). However, it is possible to account for the pattern observed in the JQ plot by assuming a single decision criterion and a change of the drift rate between “speed” and “accuracy” conditions. We compared the goodness-of-fit of the model with decision boundary dependent on instruction (whose results are shown are in Figure 5) with a diffusion model using only one value for the decision criterion but independent (linear) relations of the drift rates in “speed” and “accuracy” conditions. Using this model structure, we were able to account for overlapping JQ plot characteristics; the χ^2 values for these models are higher compared to the model structure reported in the Appendix, $t(9) = -2.3$, $p < .05$.

Conclusion

We presented a psychophysical experiment on the speed/accuracy tradeoff in human force perception. Participants judged whether a force applied to their resting hand is perceived to be “low” or “high.” A diffusion model has been fitted to the responses. The prediction error is in the range of error values reported for studies in the visual domain, suggesting that despite the difference in spatiotemporal properties of the stimuli, the diffusion model is applicable to force perception as well. However, the diffusion model fails in predicting how sensitivity in force judgments depends on response time as evidenced by a new kind of analysis called JQ plot. The JQ plot evidences the speed/accuracy pattern suggesting that sensitivity increases with response times up to 0.6 s, regardless of the experimental instruction to focus on response “accuracy” or “speed.”

The unexplained feature in the JND as a function of RT quantile gives rise to the question whether an alternative to the diffusion model could capture this phenomenon. Candidates to start with could include Bayesian observers, that is, the Kalman filter or particle filters. The Kalman Filter is a special case of a diffusion process and is capable of mimicking different established perception models as well, for example, the Ornstein-Uhlenbeck process used in other studies (P. L. Smith et al., 2014).

The novel analysis technique of the JQ plot should be further investigated. In particular, it would be interesting to see whether perceptual sensitivity increases over time and regardless of the experimental instructions in other experimental paradigms and with information coming from other sensory modalities such as vision.

References

- Bonnet, C., & Dresp, B. (1993). A fast procedure for studying conditional accuracy functions. *Behavior Research Methods, Instruments, & Computers*, 25, 2–8. <http://dx.doi.org/10.3758/BF03204443>
- Cholewiak, R. W., & Collins, A. A. (2000). The generation of vibrotactile patterns on a linear array: Influences of body site, time, and presentation mode. *Perception & Psychophysics*, 62, 1220–1235. <http://dx.doi.org/10.3758/BF03212124>
- Ernst, M. O., Lange, C., & Newell, F. N. (2007). Multisensory recognition of actively explored objects. *Canadian Journal of Experimental Psychology/Revue canadienne de psychologie expérimentale*, 61, 242–253. <http://dx.doi.org/10.1037/cjep2007025>
- Fitts, P. M. (1954). The information capacity of the human motor system in controlling the amplitude of movement. *Journal of Experimental Psychology*, 47, 381. <http://dx.doi.org/10.1037/h0055392>
- Heller, M. A. (1984). Active and passive touch: The influence of exploration time on form recognition. *The Journal of General Psychology*, 110, 243–249. <http://dx.doi.org/10.1080/00221309.1984.9709968>
- Jones, L. A. (1986). Perception of force and weight: Theory and research. *Psychological Bulletin*, 100, 29–42. <http://dx.doi.org/10.1037/0033-2909.100.1.29>
- Lederman, S. J., & Klatzky, R. L. (2009). Haptic perception: A tutorial. *Attention, Perception, & Psychophysics*, 71, 1439–1459. <http://dx.doi.org/10.3758/APP>
- Livingstone, M., & Hubel, D. (1987). Psychophysical evidence for separate channels for the perception of form, color, movement, and depth. *Journal of Neuroscience*, 7, 3416–3468.
- Luce, R. D. (1986). *Response times: Their role in inferring elementary mental organization*. New York, NY: Oxford University Press.
- Rank, M., & Di Luca, M. (2014). Response time-dependent force perception during hand movement. In M. Auvray & C. Duriez (Eds.), *Haptics: Neuroscience, devices, modeling, and applications* (pp. 85–92). Berlin, Germany: Springer. http://dx.doi.org/10.1007/978-3-662-44193-0_12
- Ratcliff, R. (1978). A theory of memory retrieval. *Psychological Review*, 85, 59–108. <http://dx.doi.org/10.1037/0033-295X.85.2.59>
- Ratcliff, R. (1993). Methods for dealing with reaction time outliers. *Psychological Bulletin*, 114, 510–532. <http://dx.doi.org/10.1037/0033-2909.114.3.510>
- Ratcliff, R. (2002). A diffusion model account of response time and accuracy in a brightness discrimination task: Fitting real data and failing to fit fake but plausible data. *Psychonomic Bulletin & Review*, 9, 278–291. <http://dx.doi.org/10.3758/BF03196283>
- Ratcliff, R. (2014). measuring psychometric functions with the diffusion model. *Journal of Experimental Psychology: Human Perception and Performance*, 40, 870–888. <http://dx.doi.org/10.1037/a0034954>
- Ratcliff, R., Gomez, P., & McKoon, G. (2004). A diffusion model account of the lexical decision task. *Psychological Review*, 111, 159–182. <http://dx.doi.org/10.1037/0033-295X.111.1.159>
- Ratcliff, R., & McKoon, G. (2008). The diffusion model: Theory and data for two-choice decision tasks. *Neural Computation*, 20, 873–922. <http://dx.doi.org/10.1162/neco.2008.12-06-420>
- Ratcliff, R., & Smith, P. L. (2010). Perceptual discrimination in static and dynamic noise: The temporal relation between perceptual encoding and decision making. *Journal of Experimental Psychology General*, 139, 70–94. <http://dx.doi.org/10.1037/a0018128>
- Ratcliff, R., Thapar, A., & McKoon, G. (2001). The effects of aging on reaction time in a signal detection task. *Psychology and Aging*, 16, 323–341. <http://dx.doi.org/10.1037/0882-7974.16.2.323>
- Ratcliff, R., & Tuerlinckx, F. (2002). Estimating parameters of the diffusion model: Approaches to dealing with contaminant reaction times and parameter variability. *Psychonomic Bulletin & Review*, 9, 438–481. <http://dx.doi.org/10.3758/BF03196302>
- Smith, P. (2000). Stochastic dynamic models of response time and accuracy: A foundational primer. *Journal of Mathematical Psychology*, 44, 408–463. <http://dx.doi.org/10.1006/jmps.1999.1260>
- Smith, P. L., Ratcliff, R., & Sewell, D. K. (2014). Modeling perceptual discrimination in dynamic noise: Time-changed diffusion and release from inhibition. *Journal of Mathematical Psychology*, 59, 95–113. <http://dx.doi.org/10.1016/j.jmp.2013.05.007>
- Swenson, R. G. (1972). The elusive tradeoff: Speed vs. accuracy in visual discrimination tasks. *Perception & Psychophysics*, 12, 16–32. <http://dx.doi.org/10.3758/BF03212837>
- Todorov, E. (2004). Optimality principles in sensorimotor control. *Nature Neuroscience*, 7, 907–915. <http://dx.doi.org/10.1038/nn1309>
- Vandekerckhove, J., & Tuerlinckx, F. (2007). Fitting the Ratcliff diffusion model to experimental data. *Psychonomic Bulletin & Review*, 14, 1011–1026. <http://dx.doi.org/10.3758/BF03193087>
- Vandekerckhove, J., & Tuerlinckx, F. (2008). Diffusion model analysis with MATLAB: A DMAT primer. *Behavior Research Methods*, 40, 61–72. <http://dx.doi.org/10.3758/BRM.40.1.61>
- Weber, E. H. (1834). *Die Lehre vom Tastsinne und Gemeingefühle auf Versuche Gegründet*. Braunschweig, Germany: Friedrich Vieweg und Sohn.
- Wichmann, F. A., & Hill, N. J. (2001). The psychometric function: I. Fitting, sampling, and goodness of fit. *Perception & Psychophysics*, 63, 1293–1313. <http://dx.doi.org/10.3758/BF03194544>
- Wickelgren, W. A. (1977). Speed-accuracy tradeoff and information processing dynamics. *Acta Psychologica*, 41, 67–85. [http://dx.doi.org/10.1016/0001-6918\(77\)90012-9](http://dx.doi.org/10.1016/0001-6918(77)90012-9)

(Appendix follows)

Appendix

Diffusion Model Fitting

For fitting the diffusion model to experimental data, grouping data from conditions with equal difference to the POE is a common technique to reduce the number of model parameters and increase the statistical power (see, e.g., Ratcliff et al., 2001). To test whether symmetric force conditions around the POE can be grouped together, their response characteristics must be symmetrical to this experimental condition as well. Participants' individual PSEs, indicating the perceived threshold between "small" and "large" forces are significantly lower than the POE being 3.3 N. As a consequence of this significant difference, a grouping of symmetric experimental conditions is not possible here. Instead, every experimental condition results in an individual set of model parameters.

Parameters are identified by minimizing the χ^2 value between the model predictions and the experimental data. The relation between physical stimulus and drift rate is often (but not always) linear as discussed in a recent paper by Ratcliff (2014). To test which drift rate function is a feasible choice, a linear function and four alternative models are tested, constraining drift rate depending on the force level and the starting point of the diffusion model as follows:

1. drift rate ν independent ($\nu_1 \dots 10 = \text{const.}$), $z = a/2$;
2. ν proportional to the force level, $z = a/2$;
3. ν proportional to the force level, a free;

4. ν follows a power function, a free; and
5. ν varies freely with each force level, a free.

All other constraints on the model parameters remain. Because these models are nested, that means, Model 1 with 7 *df* is a special case of Model 2 (8 *df*); Model 2 is a special case of Model 3 (10 *df*) and so on, a likelihood ratio test can be used to investigate whether the additional degrees of freedom justify the improvement in model fit (Vandekerckhove & Tuerlinckx, 2007). In all participants, a linear variation of drift rate with force condition (model 2) leads to significantly improved modeling accuracy ($p < 0.001$) over Model 1. Identifying the starting point as another free parameter improves the quality of fit significantly over the fixed initial point at $a/2$ in seven participants. However, only one participant's quality of fit improves significantly with the additional degrees of freedom introduced by Models 4 and 5. The identified parameter values for a model with drift rates linearly related to the force level and free starting point are summarized in Table A1. The relation between drift rate and force level is reported as

$$\nu_i = I + mf_i \quad (1)$$

where I is the intersection and m the slopes of the linear function.

Table A1
A Summary of Identified Parameters and the Final Value of the χ^2 Optimization Criterion

Subject	a_{acc}	a_{sp}	T_{er}	η	z_{acc}	z_{sp}	s_z	s_t	I	m	X^2
P1	71.6	61.1	400.5	3.6	36.8	30.5	60.1	173.5	-737.9	222.7	180.3
P2	117.5	74.3	445.2	185.3	62.3	40.8	43.9	159.7	-1,237.4	382.4	135.7
P3	107.4	61.4	455.3	240.1	49.8	30.7	27.3	183.1	-1,938.8	612.7	144.6
P4	119.4	59.1	498.1	266.3	60.7	29.6	58.1	147.4	-2,280.8	702.3	152.9
P5	96.8	54.5	461.7	249.9	41.8	26.4	0.0	162.4	-1,597.1	527.4	241.6
P6	77.3	66.0	473.0	7.9	34.7	39.3	0.0	6.7	-699.4	226.1	27.9
P7	92.6	3.4	442.0	200.0	37.3	0.6	0.5	397.8	-1,205.9	387.5	54.9
P8	79.0	61.7	423.9	195.1	45.9	34.4	52.2	189.5	-1,902.4	586.6	122.0
P9	200.3	71.9	371.0	118.7	99.7	40.5	54.0	96.3	-1,135.3	331.7	127.1
P10	83.4	62.7	425.1	189.9	46.1	37.1	19.7	208.0	-1,793.9	546.7	139.4
mean	104.5	57.6	439.6	165.7	51.5	31.0	31.6	172.4	-1,452.9	452.6	132.6
SEM	11.9	6.3	11.5	29.7	6.1	3.7	8.0	31.0	168.3	52.5	18.8

Note. acc = conditions with instruction to focus on accuracy; sp = on speed. All values in this table except χ^2 are multiplied by 1,000 for better readability.

Received February 6, 2014
Revision received December 22, 2014
Accepted January 7, 2015 ■